Spike artifact reduction in nonconvex Compressed Sensing

T. C. Basse-Luesebrink[1,2], T. Kampf[1], A. Fischer[1,3], G. Ladewig[2], G. Stoll[2], and P. M. Jakob[1,3]
[1]Experimental Physics 5, University of Wuerzburg, Wuerzburg, Germany, [2]Neurology, University of Wuerzburg, Wuerzburg, Germany, [3]Research Center for Magnetic Resonance Bavaria (MRB), Wuerzburg, Germany

Introduction

Compressed sensing (CS), a reconstruction method for undersampled MR data, was recently introduced [1]. Since only undersampled data are acquired, CS allows a significant reduction in the time needed for MR experiments. The basic requirement for CS, however, is sparsity in the data. The lack of ^{19}F background signal in living tissue leads to an intrinsically sparse signal distribution in the ^{19}F image domain. This makes ^{19}F MR a suitable application for CS [2]. However, ^{19}F MR data often suffers from a low SNR, which is problematic for CS. Thus, spike artifacts often appear highly pronounced especially in nonconvex CS reconstructions of noisy ^{19}F MR data.
The present study focuses on the reduction of spike artifacts in these CS reconstructions. Therefore, a post-processing "de-spike algorithm" is proposed, using the fact that the spatial position of spike artifacts depends on the chosen sampling pattern. Numerical phantom simulations as well as *ex-* and *in-vivo* ^{19}F CSI experiments were performed.

Materials and Methods

Simulations were performed on a numerical, simplified 3D mouse phantom. All MR measurements were performed using a ^{1}H/^{19}F birdcage coil on a 7T small animal scanner. A fixed mouse labeled with ^{19}F markers served as an *ex-vivo* phantom. Before marker application, a cerebral infarction was induced using photothrombosis. An additional animal prepared similarly as the *ex-vivo* animal was measured *in-vivo*.
For *ex-* and *in-vivo* experiments, fully sampled ^{19}F-3D-bssfp-CSI [3] experiments were performed. Imaging parameters: T_{acq}/TR = 10/13.5ms; FOV = 70x30x30mm; MTX = 70x48x48; NA = 1. Additionally, a randomly undersampled dataset with an acceleration factor (af) of 8 was acquired. All three spatial dimensions were undersampled.
In Fig. 1, the different data processing steps are displayed. First, a CS reconstruction of the undersampled data was obtained [2,4]. Second, the CS reconstructed data was inverse Fourier transformed. Third, the kspace data was multiplied with a different randomly distributed sampling pattern containing zeros and ones. Fourth, the new undersampled kspace data was Fourier transformed into the image domain and in a 5th step CS reconstructed. Steps 3-5 were repeated n times. In a final 6th step, the n CS reconstructions were used to generate averaged data. In addition, multiple filters were studied, which focused on the identification of spike artifacts from the n CS reconstructions.

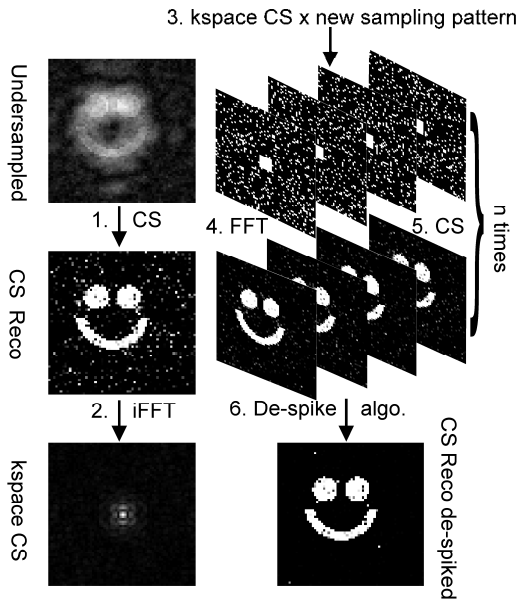

Fig.1: Scheme of the different data processing steps.

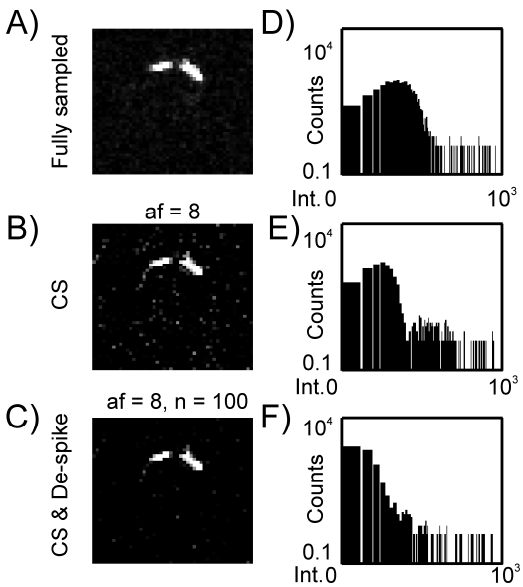

Fig.2: Results from the ex-vivo experiments of a representative slice/spectral point in the brain are shown (af=8, p=0.75). All data was scaled for better visualization of the spike artifacts. N = 100 additional CS reconstructions were performed. A) Shows the fully sampled reference, B) the CS reconstructed image, and C) the averaged data from the n = 100 CS reconstructions. D-E) show the corresponding histograms (logarithmic scale).

Results

In Fig. 2, exemplary *ex-vivo* data is displayed. The same slice and spectral point from the brain region is displayed in all images (Fig. 2A-C). Contrary to the fully sampled case (Fig. 2A), the undersampled, nonconvex CS reconstructed data shows visible spike artifacts (Fig. 2B). The histogram in Fig. 2E reflects this behavior. Furthermore, in comparison with the histogram of the fully sampled case (Fig. 2D), Fig. 2E shows that the CS algorithm modifies the signal distribution.
The averaged data generated from the n = 100 CS reconstructions are shown in Fig. 2C and 2F. Spike artifacts appear less pronounced compared to the initial CS reconstructed data. This behavior can also be observed when comparing the histograms of Fig. 2E and 2F. Again, a further modification of the signal distribution can be observed.
Phantom as well as *in-vivo* experiments provided similar results (data not shown).

Discussion and Conclusion

The proposed algorithm was able to significantly reduce spike artifacts of nonconvex CS reconstructions and thus improve image quality.
Besides simply averaging the n CS reconstructions, multiple other “de-spiking filters” can be applied in order to identify spikes in nonconvex CS reconstructions and thus further optimize image quality. Furthermore, since this algorithm is a pure post-processing method, no additional scanner time is needed.

References

[1] Lustig et al., Magn Reson Med 58:1182–1195, (2007)
[2] A. Fischer et al.; Proc. ISMRM, V.17, Abstract 3154 (2009)
[3] Speck et al., Magn Reson Med 48(4), 633-639 (2002)
[4] A. Fischer et al.; Proc. ISMRM, V.16, Abstract 1487 (2008)

Acknowledgements

This work was partly supported by the DFG SFB 688 (B1, B3, B5) and the IZKF Würzburg Project F-25.